Optik 145 (2017) 99–105

Contents lists available at ScienceDirect

Optik

journal homepage: www.elsevier.de/ijleo

Original research article

CuO nanocrystals embedded in KBr single crystal: Elaboration and characterization

Lazhar Bouhdjer*, Samyia Addala*, Ouahiba Halimi, Miloud Sebais, Boubaker Boudine

Laboratory of Crystallography, Department of Physics, University of Constantine, Constantine, 25000, Algeria

ARTICLE INFO

Article history:
Received 15 April 2017
Accepted 10 July 2017

Keywords:
KBr:CuO crystal growth
CuO nanocrystals
XRD
Raman spectroscopy
Photoluminescence

ABSTRACT

More recently, there are important number of papers which have been stimulated by the optical characteristics of crystalline matrixes doped with quantum dots (QDs), nanoparticles (NPs) or nanocrystals (NCs) of semiconductors. In this context, we suggest this investigation, which highlights the doping effects of CuO (NCs) on structural and optical properties of KBr single crystal. In this approach, we expose a simple and realizable technique for embedding CuO NCs as three dimensions (3D) defects in a KBr crystalline matrix. The Czochralski method was used to obtain a KBr:CuO single crystal starting from inhomogeneous phase melt-NCs in the crystallization melting-pot. However, the nano-regime of guest material creates a difficult challenge, because there is a possibility of fusing of the CuO NCs during the crystal growth process. Nevertheless, the whole structural results prove that the NCs inside KBr:CuO single crystal have monoclinic phase with nano-regime size. In addition, these results appear that the CuO NCs have two orientations preferred inside KBr host and demonstrate that the chemical bond Cu—O of CuO monoclinic phase steel exists. Relative to the optical properties, the UV–visible absorption spectroscopy exhibits that the NCs inside KBr:CuO sample have a nano-regime size, where the band gap shifts toward the higher energies. Furthermore, photoluminescence (PL) of KBr:CuO single crystal appears an important intensity in the visible range, this property makes this sample as a good candidate to integrate them in the optical devices which are working in the visible range.

1. Introduction

During the past few years, the nano-semiconductors have proved itself beside the bulk semiconductors and have attracted extensive attention from scientists not only for the dramatic changing of their properties as a function of size, which is so significant for fundamental research, but also for their applications in different topics of technology as nano-electronics, nano-medicine and nano-devices of renewable energy. It is well recognized that metal oxides have reached an important place in several areas of chemistry, physics and materials science. Currently, copper oxides, especially found a wide application domain in catalytic, field emissions, gas sensing, lithium batteries, and solar cells [1–5]. Naturally copper is a metal with high electrical conductivity. However, copper oxides exist in three different forms: cupric oxide (CuO), cuprous oxide (Cu_2O), and paramelaconite (Cu_4O_3) have different properties. CuO and Cu_4O_3 phases have a monoclinic and a tetragonal

* Corresponding authors.
E-mail addresses: bouhdjerlazhar@gmail.com (L. Bouhdjer), samiaaddala@gmail.com (S. Addala).

http://dx.doi.org/10.1016/j.ijleo.2017.07.034
0030-4026/

crystal structure, they are a p-type semiconductor with a relatively narrow band gap (1.2–1.9 eV), respectively [6]. While Cu_2O phase is known to be a p-type semiconductor and a large direct band gap 2–2.6 eV with cubic structure [7].

Due to the nano-size of NCs, most them used in optical experiments, are embedded in transparent matrixes [8,9]. Basically, there are two main kinds of the transparent matrixes: amorphous matrixes [10,11] and crystalline matrixes [12,13]. Concerning the last one, there are a several different kind of transparence crystalline hosts, among these matrixes, alkali halide compounds have a wide range of possible doping impurities with different concentrations. Furthermore, due to their high gap energy (10 eV) they offer a large window for optical spectroscopy studies, especially in the Uvi-Vis range. There are several studies addressed to optical properties of semiconductors NCs self-assembled in alkali halide single crystals, for example: NaCl:CuCl, NaBr:CuBr, KCl:AgCl, KBr:AgBr and KCl:Sb_2O_3, where these NCs and matrixes make a homogeneous melt during the growth process [14–18]. Tobias Otto et al., reported an investigation about the optical properties of CdTe quantum dots (QDs) embedded in various macrocrystals of salts (NaCl, KCl and KBr). However, these macrocrystals were grown from aqueous solution [19]. In addition, M. Priya et al. reported a study about dielectric properties of NCs of oxides (ZnO and CdO) dispersed in polycrystalline of (NaCl, KCl and $NaCl_{0.5}$-$KCl_{0.5}$), these polycrystalline matrixes were obtained from melting phase [20]. Recently Yujing Liu et al., conclude that the presence of CdTe QDs and polymer dots (Pdots) as guest materials inside calcite single crystals have a fluorescence lifetime longer than the ones dispersed in gel and solution [21]. In our approach we propose to elaborate alkali halide single crystals from melting phase. But nevertheless, the embedded NCs of semiconductors save their solid state in the crystallization melting-pot. But there is a challenge, because the melting point of NCs decreases when their size decreases. We have already reported investigations about the properties of NCs dispersed in alkali halide single crystals, for example: KCl:CdS, KBr:CdTe, and NaCl:CuO [22–24]. Intel now, to the best of our knowledge, no reports available on the elaboration and characterization of KBr:CuO single crystal. In this context, we recommend to investigate the doping effects of CuO NCs on the structural and optical properties of the KBr single crystals.

2. Experimental details

As a first step the starting mixture: 98 wat% of KBr powder (Aldrich ≥99% purity) was mixed with 2 wat% of CuO (Aldrich: size <50 nm). The next step: This mixture is undergone to decreasing of the temperature till the melting point of KBr (T = 734 °C). After that, the system (melt of KBr–NCs of CuO) is shifted to (T = 731 °C). This new temperature is suitable for starting the crystallization process of the KBr host. It is very interesting to note that A.H. Battez et al. [25] have already reported that the melting point of CuO NCs (30–50 nm) is 1326 °C, which means under the crystal growth conditions of KBr single crystal the CuO NCs still have solid state property. But nevertheless, there is a possibility of fusing of CuO NCs because we are working with NCs have 15.5 nm of size (see results and discussion section). When the thermodynamic equilibrium conditions are satisfied, the seed (small KBr single crystal) kept lowering until it is just immersed in the melt. At this moment the rotation motion (1 rpm) was triggered, this velocity was maintained through all the experience. We detect the beginning of crystallization process after the first few minutes (2–3 min) through appearing a shiny disk around the contact zone (seed-melt). When this condition is satisfied we activate the pulling motion with velocity in a range of 8–10 mm/h. The obtained crystal has a yellow color with disorder dark regions and macroscopic linear defects. This crystal is cleaved into samples, each with a face being parallel to the (100) plane (see Fig. 1). Regarding a pure KBr single crystal, we use the same experimental protocol. However, in this time the starting materials are only the powder of KBr. A pure KBr single crystal has colorless property.

In this investigation the diffractometer which was used is BRUKER-AXSD8 with Cu K_α radiation ($\lambda_{K_\alpha} = 1.5402$A) and a graphite filter. In addition, the Raman spectroscopy of KBr:CuO samples were carried out using a (BRUKER 'Senterra') μ–Raman spectrometer at room temperature (RT) with a wavelength of excitation is λ_{ex} = 532 nm (YAG, green). This new instrument offers an important advantage: where the deep-μ-area of analysis is possible to change. Relative to FT-IR investigation was performed with Thermo-Nicolet equipment in the 1000–400 cm^{-1} range. Optical properties were studied using a UV–visible spectrophotometer (Shimadzu, UV-3101). Furthermore, the PL was measured at RT and the samples were excited by an argon laser (ionized light Eexc = 313 nm) with an output power of 10 mW.

Fig. 1. Photograph of a KBr:CuO single crystal.

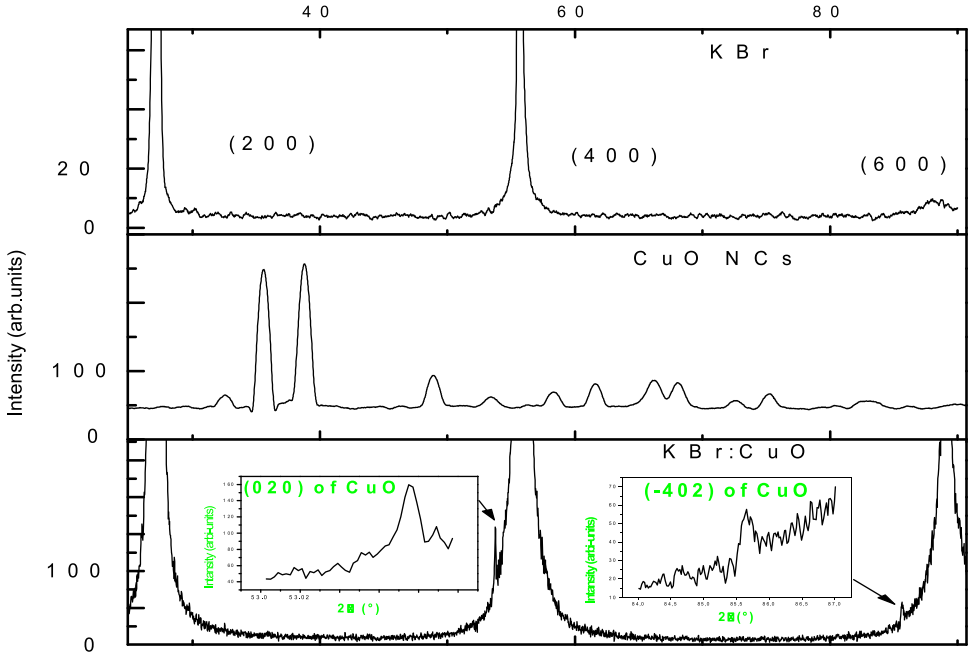

Fig. 2. The XRD pattern of: a pure KBr single crystal (faces are parallel to the (100) plane), CuO NCs, and a KBr:CuO single crystal (faces are parallel to the (100) plane).

3. Results and discussion

Fig. 2 represents XRD patterns of three different samples: a pure KBr single crystal, CuO NCs, and an KBr:CuO single crystal. From the spectrum of KBr crystal, we can see only three peaks found at: $2\theta = 27.12^{\circ}$, $2\theta = 55.70^{\circ}$, and $2\theta = 87.94^{\circ}$ correspond to the (200) plane and its harmonic planes (400) and (600), respectively. It is easy to conclude from this result that the sample has a single crystal character. Also the spectrum denotes that the sample is cleaved where the faces are parallel to the (100) plane. In addition, the absence of peaks relative to impurities indicates that the KBr single crystal has a good purity. The XRD spectrum of the CuO NCs was displayed in Fig. 2. The diffraction peaks consist with the monoclinic structure of CuO with lattice constants a = 4.69, b = 3.42, c = 5.13A, $\beta = 99^{\circ}52'$, and the C2/c symmetry space group as reported in the JCPDS 41-0254 card. Besides, the nanometric particle size translated through a broadening of the majority of peaks, Scherrer's formula was used to estimate the crystallite size of CuO which is found to be about 15.5 nm.

$$D = \frac{0.9\lambda}{B(\theta)\cos(\theta)} \tag{1}$$

Where D is the crystallite diameter, λ the wavelength, θ the Bragg angle, and B (θ) the full width at half maximum (FWHM) of the peak.

Regarding the XRD pattern of the KBr:CuO sample (see Fig. 2), there are three intense peaks related to the host (KBr), and two weak peaks located at $2\theta = 53.76^{\circ}$ and $2\theta = 85.68^{\circ}$, attributed respectively to the plans (020) and $(\bar{4}02)$of CuO monoclinic phase. However, all other peaks of CuO do not appear, and this observation donates that the crystallites of CuO display preferred orientation in these two directions, where their axes are almost parallel to the crystallographic axes of the KBr lattice. Frôhlich et al., and Haselhoff et al. [14,15] have already proved the same note, they found that the axes of CuCl NCs are parallel to the axes of the NaCl lattice and KCl lattice, respectively. As is well known that the melting point of NCs decreases when their size decreases [26]. This fact makes a challenge for what we postulate in the beginning. Nevertheless, the XRD spectrum of KBr:CuO harmonious with the postulate: where the absence of peaks relative to other phases, such as K_2CuBr_3, proving that the CuO NCs still have their solid state properties during the crystal growth process. In addition, the estimated of the average size of CuO NCs inside KBr is almost triple times (47.84 nm) as compared with that of CuO nanopowder (15.50 nm). Basing on the fact, that the Gibbs free energy of the surface of NCs is usually high, and the NCs have the tendency toward aggregate formation, thereby reducing the Gibbs free energy of the surface [27]. We speculate that available conditions in the crystal growth environment contribute to the agglomeration process of CuO NCs. The resulting sizes of CuO NCs are listed in Table 1.

Usually, Raman spectroscopy uses to investigate the structural properties of nanomaterials [28,29]. Fig. 3 shows the Raman spectrum of KBr:CuO at RT with different deep area μ-analysis. It can be seen from this curve three Ramans modes ($A_g + 2B_g$) located at 297, 334 and 608 cm^{-1} attributed to the CuO monoclinic phase, which is consistent with XRD analysis.

Table 1
Crystallites sizes calculated from the XRD.

2θ (°)	53.76	85.68
(hkl)	(020)	$(\bar{4}02)$
β(°)	0.174	0.24
D (nm)	50.56	45.13

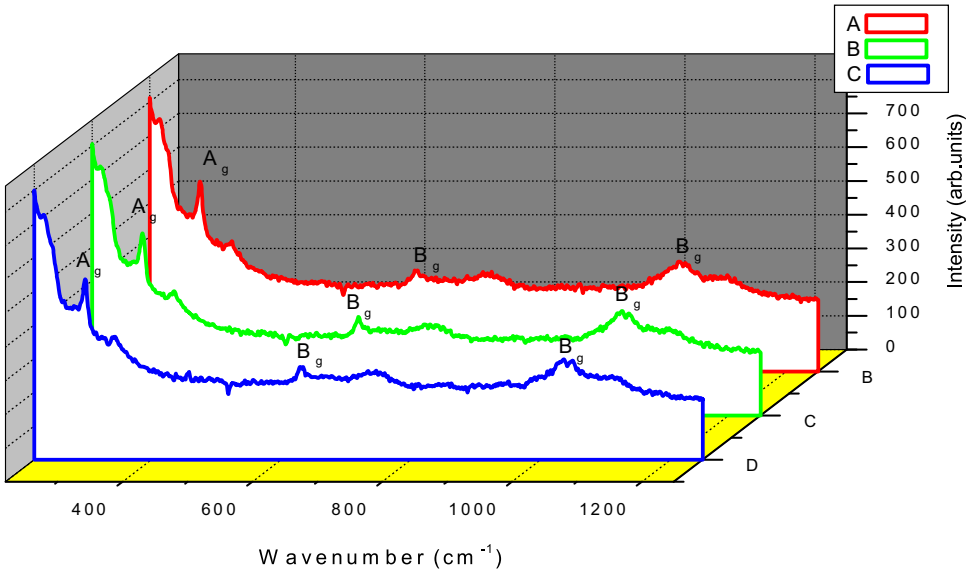

Fig. 3. Raman spectrum of KBr:CuO: (A) The area μ-analysis is on the surface of the sample. (B) Deep of the area μ-analysis exists under 0.5 μm of the surface and (C) Deep of the area μ-analysis exists under 1 μm of the surface.

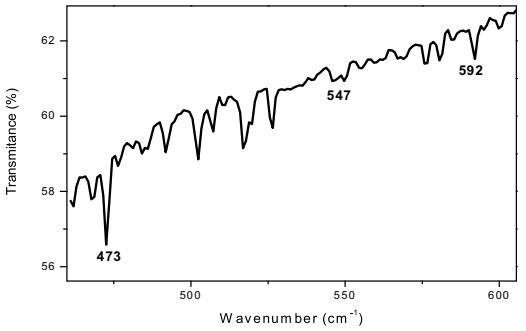

Fig. 4. FT-IR spectra of pure KBr:CuO.

These peaks are largely reported in the literature [30–32]. The intensity of beaks (Figue 3) is reduced with increasing of deep of the area which was analyzed due to the constraint exerted by the KBr host.

In the older generations of IR spectrometry usually they use alkali halide compounds as support, because these compounds are transparent in the IR range. Fig. 4 displays the FT-IR transmission spectra of KBr:CuO crystal. Though, the FT-IR spectrum of KBr:CuO in Fig. 4 shows three peaks situated at 473, 547, and 592 cm^{-1} respectively, which are characteristics of vibrations along the Cu—O bond. [33,34]. These outcomes confirm the inclusion of the monoclinic CuO phase in the KBr host.

The optical absorption spectrum of a pure KBr crystal represented in Fig. 5 (a), shows that KBr has a strong absorption near ultraviolet and it is transparent in the visible region. On the other hand, the optical band gap determined by the minimum of second derivative method [35] is E_{gKBr} = 6.2 eV (see insert Fig. 5 (a)).

In other side, the sample of KBr:CuO exhibits tow absorption bands centered around 465 nm and 625 nm. The first one attributed to the allowed direct transitions which are dominant in the CuO NCs, where the band gap appears a significant amount of blue shift (ΔE gap = 0.85 eV) toward high energies, as compared to the band gap of bulk CuO [36]. This blue-shift is caused by the well-known quantum confinement effect. Although, the average size CuO NCs inside KBr crystal is about 47.84 nm is larger double times of the Bohr radius of CuO semiconductor (R_B = 28.7 nm) [37], but there are interesting effects due to the confinement of translational motion of the whole exciton. Returning to the second band, it is relative to color

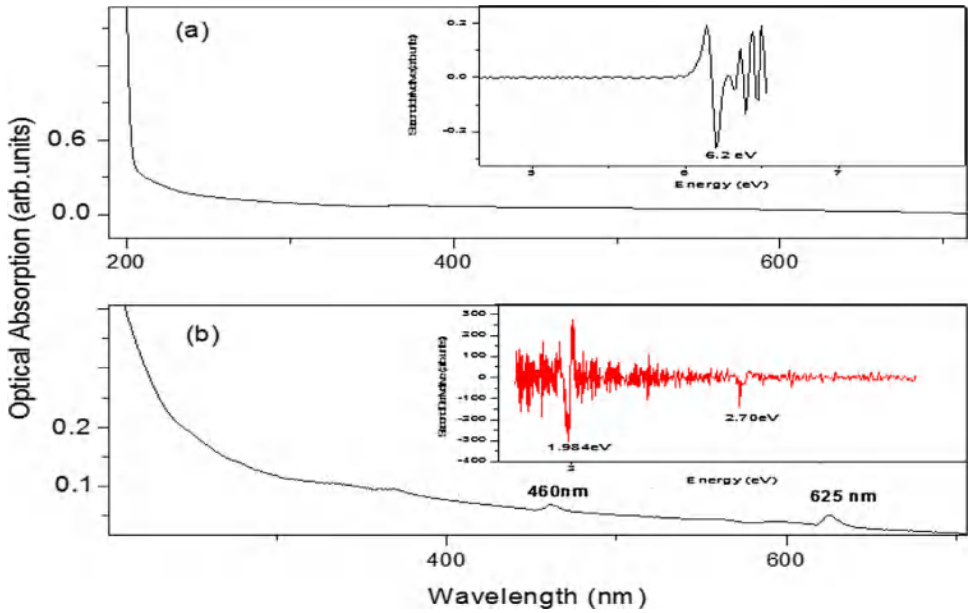

Fig. 5. (a) Optical absorption spectrum of the pure KBr crystal with E_g of the KBr crystal and (b) Optical absorption spectrum of the pure KBr:CuO crystal with E_g of the CuO NCs inside KBr crystal.

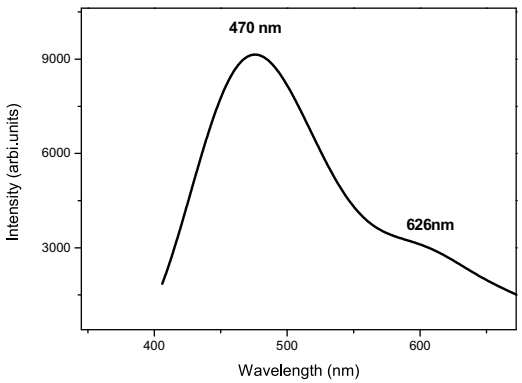

Fig. 6. Photoluminescence spectrum of a KBr:CuO crystal.

center type-F [38]. This result leads us to think that the including of CuO NCs stimulates other punctual defects such as color center.

As a coincidence result with optical absorption property, the photoluminescence (PL) exhibits two bands located at 470 nm and 626 nm (see Fig. 6). The first band (470 nm) originates from the allowed direct transitions of carrier charges in the CuO NCs. A similar result is obtained by X. Zhao et al. [39] who observed an emission band centered at 465 nm for a CuO nanowire with a size of 85 nm when the excitation wavelength was 370 nm. Furthermore, The high intensity makes this sample a good candidate for integrate them in optical devices those active in the visible range. In addition, the weak band found at 626 nm is attributed to the color center type-F.

4. Conclusion

In the present work, we report an experimental study contain a preparation, structural and optical characterization of KBr single crystal doped with CuO nanocrystals (NCs) as bulk defects. KBr and KBr:CuO single crystals are growing by the Czochralski method along [100] crystallographic axes. In order to characterize the samples with comfortably, the obtained crystals are cleaved parallel to the (100) face with suitable size. The XRD results indicate that the KBr and KBr:CuO have a single crystal character with high purity. In addition, the estimated size of CuO crystallites in KBr:CuO crystal is about 47.48 nm and the orientation of CuO NCs have only two directions preferred (020) and $(\bar{4}02)$. In other side, Raman spectroscopy and Fourier transform infrared (FT-IR) confirm the existence of Cu-O chemical liaison in the CuO monoclinic phase. Regarding the optical properties, the Uvi-Vis absorption exhibited a bond absorption located at 460 nm (1.98 eV)

due to the allowed direct transitions of CuO NCs. The nano-size of doping CuO translated by exhibiting a blue shift of the gap (ΔE gap = 0.85 eV) toward the higher energies. Furthermore, Photoluminuscence (PL) spectroscopy appear a large and intense band located at around 438 nm (eV) due to CuO NCs, which supported these samples to introduce them in optical devises active in the visible range. The whole results prove that the elaboration of KBr:CuO single crystal starting from inhomogeneous melt phase has been achieved, where the CuO NCs keep their properties.

Acknowledgment

This project supported by the Crystallography Laboratory of the University of Constantine, Algeria.

References

[1] S. Govindasamy, T. Marimuthu, M.S. Vaiyazhipalayam, Optical, catalytic and antibacterial properties of phytofabricated CuO nanoparticles using *Tecoma castanifolia* leaf extract, Optik 127 (2016) 7822–7828.
[2] Y.W. Zhu, T. Yu, F.C. Cheong, X.J. Xu, C.T. Lim, V.B.C. Tan, et al., Large-scale synthesis and field emission properties of vertically oriented CuO nanowire films, Nanotechnology 16 (2005) 88–92.
[3] Jiatao Zhang, Junfeng Liu, Qing Peng, Xun Wang, Yadong Li, Nearly monodisperse Cu_2O and CuO nanospheres: preparation and applications for sensitive gas sensors, Chem. Mater. 18 (2006) 867–871.
[4] Shuyan Gao, Shuxia Yang, Jie Shu, Shuxia Zhang, Zhengdao Li, Kai Jiang, Green fabrication of hierarchical CuO hollow micro/nanostructures and enhanced performance as electrode materials for lithium-ion batteries, J. Phys. Chem. C 112 (2008) 19324–19328.
[5] Sajad Hussain, Chuanbao Cao, Ghulam Nabi, Waheed S. Khan, Muhammad Tahir, Muhammad Tanveer, Optical and electrical characterization of ZnO/CuO heterojunction solar cells, Optik 130 (2017) 372–377.
[6] B.K. Meyer, A. Polity, D. Reppin, et al., Binary copper oxide semiconductors: from materials towards devices, Phys. Status Solidi B 249 (2012) 1487–1509.
[7] H. Markus, E. Bianca, H. Christian, Band structure and phase stability of the copper oxides Cu_2O CuO, and Cu_4O_3, Phys. Rev. B 87 (2013) 115111.
[8] Shun-Chieh Hsu, Yin-Han Chen, Zong-Yi Tu, et al., Highly stable and efficient hybrid quantum dot light-emitting diodes, IEEE Photonics J. 7 (2015) 1601210.
[9] Marcus Adam, Nikolai Gaponik, Alexander Eychmüller, Talha Erdem, Zeliha Soran-Erdem, Hilmi Volkan Demir, Colloidal nanocrystals embedded in macrocrystals: methods and applications, J. Phys. Chem. Lett. 7 (2016) 4117–4123.
[10] W. Widanartoa, M.R. Sahar, S.K. Ghoshal, R. Arifin, M.S. Rohani, K. Hamzah, M. Jandra, Natural Fe_3O_4 nanoparticles embedded zinc-tellurite glasses: Polarizability and optical properties, Mater. Chem. Phys. 138 (2013) 174–178.
[11] Heqing Yang, Xingjun Wang, Huazhong Shi, Songhai Xie, Fujian Wang, Xiaoxiao Gu, Xi Yao, Photoluminescence of Ge nanoparticles embedded in SiO_2 glasses fabricated by a sol-gel method, Appl. Phys. Lett. 81 (2002) 5144.
[12] O. Husberg, H. Vogelsang, W. von der Osten, Confined excitons in AgI nanocrystals in crystalline KI matrix, J. Lumin. 96 (2002) 155.
[13] H. Vogelsang, O. Husberg, U. Köhler, W. von der Osten, A.P. Marchetti, Exciton self-trapping in AgCl nanocrystals, Phys. Rev. B 61 (2000) 1847.
[14] D. Fröhlich, M. Haselhoff, K. Reimann, Determination of the orientation of CuCl nanocrystals in a NaCl matrix, Solid State Commun. 94 (1995) 189.
[15] M. Haselhoff, H. Weber, Nanocrystal growth in alkali halides observed by exciton spectroscopy, Phy. Rev. B 58 (1998) 5052.
[16] P.G. Baranov, N.G. Romanov, V.A. Khramtsov, V.S. Vikhnin, Oriented silver chloride microcrystals and nanocrystals embedded in a crystalline KCl matrix, as studied by means of electron paramagnetic resonance and optically detected magnetic resonance, J. Phys. Condens. Matter. 13 (2001) 2651.
[17] P.G. Baranov, N.G. Romanov, V.L. Preobrazhenskiĭ, V.A. Khramtsov, Electron-Hole Recombination Confinement in Self-Organized AgBr Nanocrystals in a Crystalline KBr Matrix, JETP Lett. 76 (2002) 465–468.
[18] L. Bouhdjer, S. Addala, A. Chala, O. Halimi, B. Boudine, M. Sebais, Elaboration and characterization of a KCl single crystal doped with nanocrystals of a Sb_2O_3 semiconductor, J. Semicond. 34 (2013) 043001.
[19] Tobias Otto, Marcus Müller, Paul Mundra, Vladimir Lesnyak, Hilmi Volkan Demir, Nikolai Gaponik, Alexander Eychmüller, Colloidal nanocrystals embedded in macrocrystals: robustness, photostability, and color purity, Nano Lett. 12 (2012) 5348–5354.
[20] M. Priya, C.K. Mahadevan, Preparation and dielectric properties of oxide added NaCl?KCl polycrystals, Phys. B 403 (2008) 67–74.
[21] Yujing Liu, Huidong Zang, Ling Wang, Weifei Fu, et al., Nanoparticles incorporated inside single-Crystals: enhanced fluorescent properties, Chem. Mater. 28 (2016) 7537–7543.
[22] B. Boudinea, M. Sebaisa, O. Halimia, R. Mourasb, A. Boudriouab, P. Boursonb, Characterization of CdS nanocrystals embedded in KCl single crystal matrix grown by Czochralski method, J. Opt. Mater. 25 (2004) 373–377.
[23] A. Bensouicia, J.L. Plazab, E. Diéguezb, O. Halimia, B. Boudinea, S. Addalaa, L. Guerbousc, M. Sebais, CdTe aggregates in KBr crystalline matrix, J. Lumin. 129 (2009) 948–951.
[24] S. Addala, L. Bouhdjer, A. Chala, A. Bouhdjar, O. Halimi, B. Boudine, M. Sebais, Structural and optical properties of a NaCl single crystal doped with CuO nanocrystals, Chin. Phys. B 22 (2013) 098103.
[25] A.H. Battez, R. Gonàlez, J.L. Viesca, J.E. Fernàndez, J.M. Dîaz Fernàndez, A. Machado, R. Chou, CuO, ZrO_2 and ZnO nanoparticles as antiwear additive in oil lubricants, J. Riba. Wear. 265 (2008) 422–428.
[26] Emil Roduner, Size matters: why nanomaterials are different, Chem. Soc. Rev. 35 (2006) 583–592.
[27] J. Zhu, H. Chan, H. Liu, X. Yang, L. Lu, X. Wang, Needle-shaped nanocrystalline CuO prepared by liquid hydrolysis of $Cu(OAc)_2$, Mater. Sci. Eng. A 384 (2004) 172.
[28] Gwénaël Gouadec, Philippe Colomban, Raman spectroscopy of nanomaterials: how spectra relate to disorder, particle size and mechanical properties, Prog. Crys. Growth Charact. Mater. 53 (2007) 1–56.
[29] Qiaobao Zhang, Kaili Zhang, Daguo Xu, Guangcheng Yang, Hui Huang, Fude Nie, Chenmin Liu, Shihe Yang, CuO nanostructures: synthesis, characterization, growth mechanisms, fundamental properties, and applications, Prog. Mater. Sci. 60 (2014) 208–337.
[30] A.S. Zoolfakar, R.A. Rani, A.J. Morfa, A.P. O'Mullane, K.K. Zadeh, Nanostructured copper oxide semiconductors: a perspective on materials, synthesis methods and applications, J. Mater. Chem. C 2 (2014) 5247.
[31] M.A. Dara, Q. Ahsanulhaq, Y.S. Kim, J.M. Sohn, W.B. Kim, H.S. Shin, Versatile synthesis of rectangular shaped nanobat-like CuO nanostructures by hydrothermal method; structural properties and growth mechanism, Appl. Surf. Sci. 255 (2009) 6279–6284.
[32] N. Mukherjee, B. Show, S.K. Maji, U. Madhu, S.K. Bhar, B.C. Mitra, G.I. Khan, A. Mondal, CuO nano-whiskers: electrodeposition, Raman analysis, photoluminescence study and photocatalytic activity, Mater. Lett. 65 (2011) 3248–3250.
[33] Kavita Borgohain, J.B. Singh, M.V. Rama Rao, T. Shripathi, Shailaja Mahamuni, Quantum size effects in CuO nanoparticles, Phys. Rev. B 61 (2000) 11093.
[34] M.A. Dar, Y.S. Kim, W.B. Kim, J.M. Sohn, H.S. Shin, Structural and magnetic properties of CuO nanoneedles synthesized by hydrothermal method, Appl. Surf. Sci. 254 (2008) 7477.
[35] O. Halimi, B. Boudine, M. Sebaisa, A. Chellouche, R. Mouras, A. Boudrioua, Structural and optical characterisation of ZnO nanocrystals embedded in bulk KBr single crystal, Mater. Sci. Engine. C 23 (2003) 1111–1114.

[36] K. Santra, C.K. Sarka, M.K. Mukherjee, B. Cosh, Thin Solid Films 213 (1992) 226.
[37] A.Mumtaz Shama Rehman, S.K. Hasanain, Size effects on the magnetic and optical properties of CuO nanoparticles, J. Nanopart. Res. 13 (2011) 2497–2507.
[38] K. Yasuhiro, H. Masamitsu, U. Masayasu, Transient formation of color centres in KBr crystals under the pulsed electron beam, J. Phys. Soc. Jpn. 33 (1972) 151–157.
[39] Xinhong Zhao, Peng Wang, Zaoxue Yan, Naifei Ren, Room temperature photoluminescence properties of CuO nanowire arrays, Opt. Mater. 42 (2015) 544–547.